Rare Metal Materials and Engineering
Volume 52, Issue 2, February 2023
Available online at www.rmme.ac.cn

Science Press

Cite this article as: Yang Shumin, Xie Bin, Zhang Wei, et al. Effect of Etching Time of ITO Targets on Electrical and Optical Properties of Deposited ITO Films[J]. Rare Metal Materials and Engineering, 2023, 52(02): 478-485.

ARTICLE

Effect of Etching Time of ITO Targets on Electrical and Optical Properties of Deposited ITO Films

Yang Shumin, Xie Bin, Zhang Wei, Kong Weijing

School of Physics and Electrical Engineering, Kashi University, Kashi 844006, China

Abstract: The formation process of nodules (small black projections) on the surface of tin-doped In_2O_3 (ITO) targets during magnetron sputtering was studied by observing the surface morphologies of ITO films prepared within etching time of 2−50 h. The effects of etching time on the electrical and optical properties of the deposited ITO films were explored. Results show that the distribution of In and Sn on the surfaces of the ITO targets changes with the etching time, resulting in uneven ITO films. The electrical and optical properties of the films are degraded significantly due to nodule formation. The photoelectric properties of the ITO films are not affected significantly by etching time within 40 h. However, a rapid deterioration is recorded when longer etching time is applied.

Key words: ITO target; ITO film; nodule; etching time; magnetron sputtering

Tin-doped In_2O_3 (ITO) film exhibits excellent electrical and optical properties as a conductive and transparent material for photoelectron component applications, such as flat panel and liquid crystal displays, solar cells, and organic light-emitting diodes. For the industrial fabrication of such types of thin films, magnetron sputtering is considered a mature method that has the comparative advantages of controllable parameters, good film uniformity, and film formation on a large area of substrate[1–6]. However, when the ITO thin films are prepared by this method, many small black projections, called "nodules", are formed on the surface of the ITO target, covering the surface near the center of the target that is etched runway. For example, Nakashima et al[7] studied the influence of the dispersion conditions of tin oxide on the nodulation formation on ITO sputtering targets. The dispersion conditions of the tin oxide are significantly improved by finer powder and enhanced mixing process. Compared with the conventional target, the modified target exhibits less nodular formation and arc initiation. In another interesting work, Omata et al[8] studied 8 different ITO targets with various Sn doping ratios, and found that for the samples with a relative density greater than 99.5%, due to local deviations from a uniform distribution of tin ions and oxygen vacancies, the local conductive electron density is uneven, thus increasing the formation rate of the nodulation. As the nodules expand and nodular density increases, the arcing effect is also intensified, the sputtering becomes unstable, and the sputtering rate decreases[7–8]. As a result, the sputtering process must be stopped to allow cleaning of the target surface, which seriously restricts the preparation efficiency of ITO films and prevents continuous production. However, the correlations of such adverse effects with the etching time have seldom been investigated, and systematically quantitative analysis about the influence of the etching time on both the electrical and optical properties of the deposited ITO films is rarely reported.

Therefore, in this study, ITO target was sputtered with the etching time of 2, 10, 20, 30, 40 and 50 h. To provide reference for the actual production of ITO film, the process of nodular formation on the surface of ITO target during magnetron sputtering was studied, and the influence of etching time on the electrical and optical properties of the deposited ITO film was discussed.

1 Experiment

The industrial ITO targets with a relative density of 99.8% was used. ITO targets were sputtered to prepare ITO film. The sputtering processes were carried out with the following fixed parameters: sputtering pressure 0.4 Pa, target base distance 50

Received date: May 13, 2022
Foundation item: Natural Science Foundation of Xinjiang Province (2020D01A08)
Corresponding author: Yang Shumin, Ph. D., Professor, School of Physics and Electrical Engineering, Kashi University, Kashi 844006, P. R. China, Tel: 0086-998-2309280, E-mail: shumin6666@126.com

mm, argon flow rate 40 mL/min (under standard state, i.e. 101 325 Pa and 273.15 K), sputtering time 5 min, and substrate temperature 300 °C. The six samples (ITO films) used were prepared when ITO target was sputtered for 2, 10, 20, 30, 40 and 50 h, named as A–F, respectively. Surface morphology of the ITO films was characterized by atomic force microscopy (AFM) and scanning electron microscopy (SEM), and the surface morphology of the ITO targets was characterized by SEM. The chemical state of ITO films was analyzed by X-ray photoelectron spectroscopy (XPS), and the phase structure and the preferred orientation of the ITO films were determined by X-ray diffraction (XRD). The resistivity, carrier concentration, and mobility of the ITO films were measured with a Hall test system. Ultraviolet-visible (UV-VIS) spectroscopy was used to measure the light transmittance of the ITO films near the visible wavelength region (300–800 nm).

2 Results and Discussion

2.1 Surface morphologies of ITO targets and ITO films

2.1.1 Surfaces of ITO target

Fig.1 shows SEM images of surfaces of the ITO target with various etching time. Fig.1a shows that when the etching time is 2 h, the target surface is relatively smooth and basically unchanged. When the etching time increases to 10 h, the target surface gradually shows tiny nodules, about 15 μm (Fig. 1b). When the etching time increases to 20 h, the nodules increase gradually and begin to develop on the target surface, and the average size of nodules is about 32 μm (Fig. 1c). When the etching time increases to 30 h, the nodule number increases significantly, with an average size of about 60 μm (Fig. 1d). When the etching time increases to 40 h, the number of nodules further increases, and the average size of nodules further increases to 105 μm (Fig. 1e). When the etching time further increases to 50 h, due to the large number of nodules, the size of nodules increases rapidly, and some nodules are adhered together to form a nodular group. The average size of nodules is 135 μm (Fig. 1f). This indicates that with the increase in etching time, nodules gradually form on the surface of ITO target. The longer the etching time, the more nodules on ITO target, and the more uniform the nodules cluster.

There are several mechanisms that can be used to understand the formation of these nodules. During the process of coating via sputtering, due to the thermal conduction barrier, the high local instantaneous temperature on the surface of the target leads to a decomposition reaction of In_2O_3 and the formation of In_2O and O_2. Black In_2O crystals are deposited on the surface of the target, which leads to the formation of small bumps (nodules). The interior of the nodules is relatively loose and porous, and the heat conduction and electrical conductivity properties of the target are degraded. Ar^+ cause a collision effect, whereas the impact energy is converted into heat, which is accumulated at the nodulation sites, further promoting the decomposition of In_2O_3. Hence, the electron motion trajectory for sputtering in the affected areas is limited, resulting in a decrease in the local sputtering rates and a shielding effect on the ITO target[9–10].

2.1.2 Surface roughness of ITO films

The particle sizes are tabulated in Table 1 and the AFM images are shown in Fig. 2. As the sputtering processes proceed, the average particle size and the surface roughness of the ITO films change significantly. As etching time increases from 2 h to 50 h, the average particle size increases from 46.76 nm to 88.49 nm, and the related RMS surface roughness increases from 2.32 nm to 5.82 nm. In addition, the surface morphologies of the ITO thin films on the target surface become rougher as the etching time increases. Notably, there is an abnormal increase of nodule at 50 h, at which the

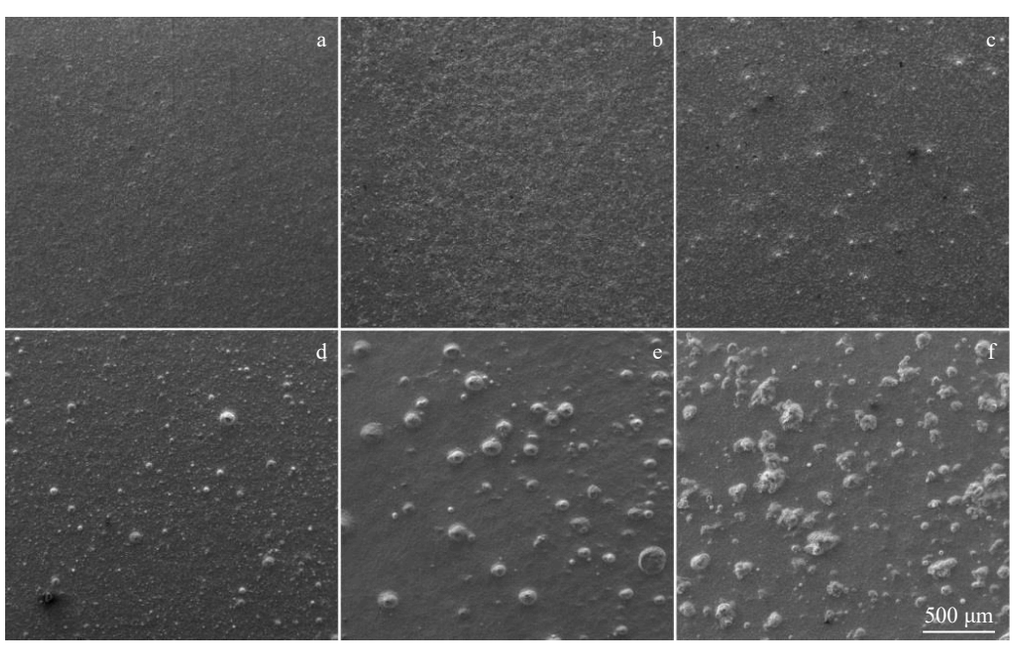

Fig.1 SEM images of surfaces of the ITO target with various etching time: (a) 2 h, (b) 10 h, (c) 20 h, (d) 30 h, (e) 40 h, and (f) 50 h

Table 1 Averaged grain size and RMS surface roughness of ITO film samples with various etching time

Etching time/h	Averaged grain size/nm	RMS surface roughness/nm
2	46.76	2.32
10	47.4	2.72
20	58.4	2.91
30	65.00	3.15
40	73.2	4.04
50	88.49	5.82

nodulation of the target is substantial, and different nodules are accumulated and connected, forming nodule groups. There are two possible explanations for this phenomenon. First, some areas shielded by nodulation on the ITO target surface are not accessible to Ar^+ sputtering, resulting in an uneven deposition of sputtered particles on the substrate. Second, when there is serious nodulation of ITO target, more large-sized particles are sputtered out. These particles will not only deposit on the surface of the ITO target to form more nodules, but also impose the formation of irregular structures on the surface of the ITO film. The resultant uneven roughness affects the resistivity and transmittance of the ITO films[9–10].

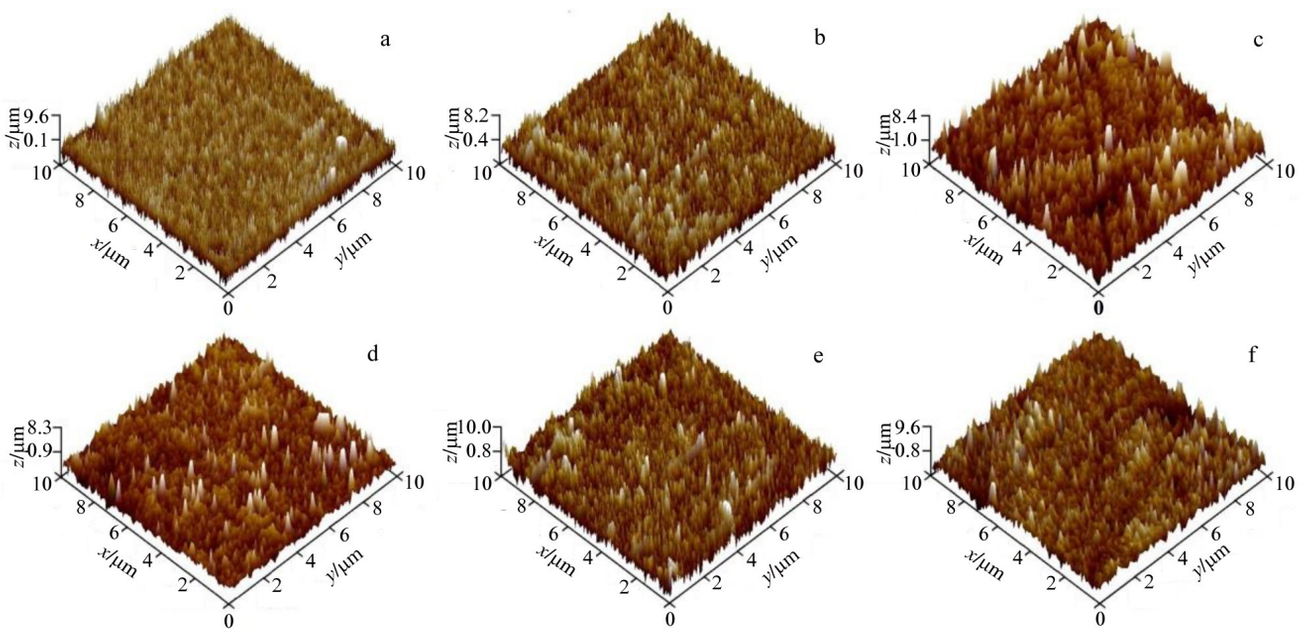

Fig.2 AFM images of ITO films with various etching time: (a) 2 h, (b) 10 h, (c) 20 h, (d) 30 h, (e) 40 h, and (f) 50 h

2.2 Influence of sputtering time on photoelectric properties of ITO films

2.2.1 Changes in resistivity, carrier concentration, and mobility of ITO films

As etching time increases (Fig. 3), the ITO films exhibit increased resistivity, and decreased mobility and carrier concentration. The resistivity, mobility, and carrier concentration change slightly within 40 h, but are significantly impacted when the etching time is 50 h.

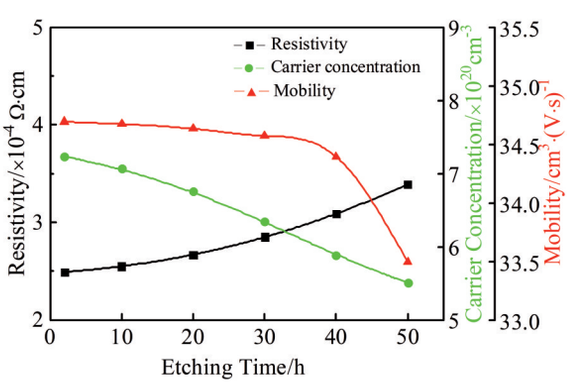

Fig.3 Resistivity, carrier concentration and mobility of ITO films with various etching time

In order to thoroughly investigate the influence of the etching time on the conductivity of ITO films at greater depth, the chemical state changes of the ITO target and the ITO film elements were further studied with different etching time.

The content ratios of In, Sn, and O elements in the nodular areas of the ITO targets are listed in Table 2. The O content in the nodulation decreases, and the Sn/(Sn+In) ratios increase gradually with the etching time, indicating that a decomposition reaction occurs. It is well-established that after the sputtering process, the high-valence oxide in the outer surface area of the target will undergo a decomposition reaction, generating a low-valence oxide (i.e. In_2O and SnO)[8,11–12]. These low-valence oxides have high resistivity, which will locate at the core of a nodular element, and are the most senior general to dozens of micron in thickness in addition to more oxygen defects. According to Lippens et al's research[13], different

Table 2 Chemical composition in the nodule with various etching time (wt%)

Etching time/h	In		Sn		Sn/(Sn+In)		O	
	Nodule	Next to nodule	Nodule	Next to nodule	Nodule	Next to nodule	Nodule	Next to nodule
2	-	-	-	-	-	-	-	-
10	86.62	88.97	3.45	3.44	0.038	0.037	9.90	10.36
20	87.59	90.74	4.26	4.23	0.046	0.045	9.62	9.87
30	88.29	92.55	4.85	4.80	0.052	0.049	9.44	9.73
40	89.43	94.81	5.14	5.10	0.054	0.051	9.32	9.60
50	91.53	97.96	5.52	5.46	0.057	0.052	9.31	9.45

phases in the ITO target have different sputtering rates, while the sputtering rate of In_2O_3 is higher than that of SnO_2, which can explain the increased concentration of Sn on the nodules.

Fig. 4 shows the XRD patterns of ITO films with different etching time, and Table 3 shows the intensity ratio of the peak (222) to the peak (400) of ITO film with various etching time ($I_{(222)}/I_{(400)}$). As etching time increases, the diffraction intensity of the (222) peak increases, and the relative diffraction intensity of the (222) peak to the (400) peak also gradually increases from 2.09 to 3.58, which indicates that ITO film preferentially forms the (222) peak with longer etching time. The change of $I_{(222)}/I_{(400)}$ of ITO film may be related to the nodules of ITO target. The nodules of the target increase with the etching time. As can be seen from Table 2, the appearance of nodules leads to a certain inhomogeneity of In and Sn on the target surface near the nodules. The inhomogeneity of In and Sn chemical components on the target surface near the nodules further affects the distribution of In and Sn chemical components in ITO films. In general, when the content of In^{3+} in ITO films is high, the crystal structure tends to form the peak (222). When Sn^{4+} content is high, the peak (400) tends to form[14–16]. According to the model proposed by Frank-Kostlin[17], two doped Sn^{4+} can bind one extra oxygen in the lattice gap nearby it. When Sn element replaces the In element in the lattice of In_2O_3, it will contribute an electron of the conduction band and generate oxygen vacancy in a certain anoxic state. The higher the content of In^{3+} and O^{2-}, the easier the indium oxide lattice formation and the less the reduced oxygen vacancies in the film, leading to the decrease of electrical properties of ITO film. Therefore, with the extension

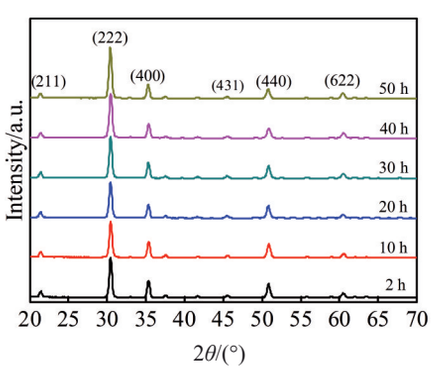

Fig.4 XRD patterns of ITO films with various etching time

Table 3 XRD pattern intensity of ITO films with various etching time

Etching time/h	(400) peak		(222) peak		$I_{(222)}/I_{(400)}$
	$I_{(400)}$	$\Delta I_{(400)}$/%	$I_{(222)}$	$\Delta I_{(222)}$/%	
2	8 023		16 820		2.09
10	7 825	−2.46	16 935	0.68	2.16
20	7 610	−2.75	18 767	10.82	2.47
30	7 249	−4.74	19 428	3.52	2.68
40	6 738.4	−7.04	21 135	8.79	3.14
50	6 643	−1.42	23 806	12.64	3.58

of etching time, the ratio of $I_{(222)}/I_{(400)}$ gradually increases, indicating that the crystal structure of ITO film tends to prefer the peak (222). The In^{3+} content increases and the oxygen vacancy decreases, resulting in the resistivity of ITO film gradually increasing from 2.49×10^{-4} Ω·cm to 4.38×10^{-4} Ω·cm.

To further explore the specific distribution of each major element in ITO films, XPS spectra are recorded to analyze the chemical states of O, Sn, and In. The obtained spectra were calibrated to the line surface impurity of the C 1s photoelectron with the binding energy of 284.6 eV. Peak-splitting and peak-fitting of the XPS spectra were performed using the Gaussian function GL(20). Fig. 5 shows the XPS spectra of ITO films deposited with different etching time, and the chemical states of each element corresponding to each energy spectrum peak. As can be seen in Fig. 5, there are only three elements In, Sn and O in the film, which are consistent with the elements in the target. The integrated areas corresponding to each element in ITO films prepared at different etching time are finally obtained through peak segmentation, fitting and calculation, and the corresponding ratios are the respective atomic ratios, with specific values shown in Table 4. It can be seen from Table 4 that the atomic ratio of In:Sn:O changes from 10: 0.925: 15.57 (at%) to 10: 0.89: 16.38, indicating that oxygen vacancies in ITO films gradually decrease with the increase in etching time during sputtering.

In order to discuss the influence of the chemical states of Sn and In on the electrical properties of ITO films, the In $3d_{5/2}$ and Sn $3d_{5/2}$ photoelectron spectra peaks of ITO films were peak-separated, as shown in Fig. 6 and Fig. 7, respectively. Here, In $3d_{5/2}$ and Sn $3d_{5/2}$ are decomposed into In $3d_{5/2}$ (I) and In $3d_{5/2}$ (II), Sn $3d_{5/2}$ (I) and Sn $3d_{5/2}$ (II), respectively. In $3d_{5/2}$ (II) and Sn $3d_{5/2}$ (II) are the high valence parts of In^{3+} and Sn^{4+}

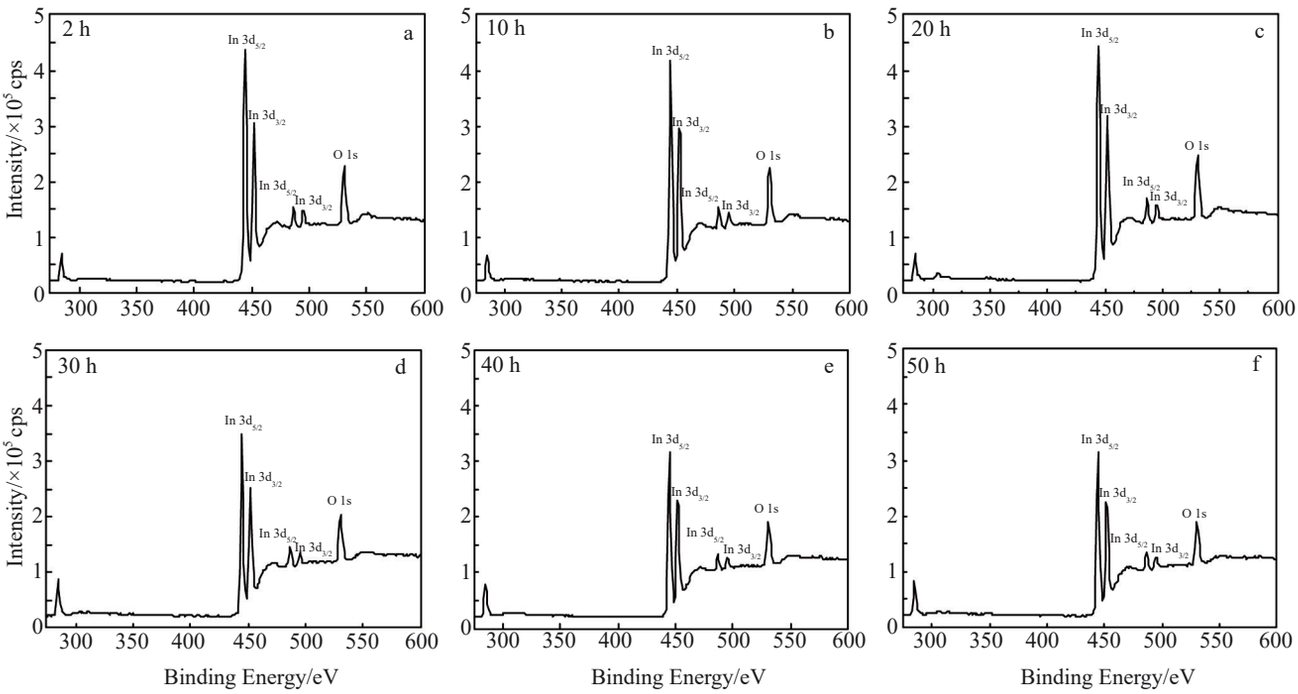

Fig.5 XPS survey spectra of ITO films with various etching time: (a) 2 h, (b) 10 h, (c) 20 h, (d) 30 h, (e) 40 h, and (f) 50 h

Table 4 Element contents in ITO films with various etching time (at%)

Element	Etching time/h					
	2	10	20	30	40	50
In	10	10	10	10	10	10
Sn	0.925	0.916	0.915	0.911	0.905	0.89
O	15.57	15.76	16.05	16.16	16.32	16.38

of ITO film, and In $3d_{5/2}$ (I) and Sn $3d_{5/2}$ (I) are the low valence parts of In and Sn of ITO film, respectively. Table 5 shows the relative content of Sn^{4+} and In^{3+} in ITO films prepared with different etching time calculated according to Fig.6 and Fig.7. As can be seen from Table 5, the relative content of In^{3+} in ITO film increases gradually, while that of Sn^{4+} decreases gradually. As the etching time is extended, the main component of the film is In^{3+}, and the number of oxygen vacancies in the film decreases gradually, causing a degradation of the electrical properties of the ITO films[18].

Fig. 8 shows the O 1s spectrum of ITO films at different etching time. O 1s can be decomposed into two peaks, i.e. O 1s (I) and O 1s (II), whose positions are basically the same, about 530.1 and 532.2 eV, respectively. O 1s (I) represents the oxygen sufficient state (oxygen state satisfying the chemical ratio) in the film, namely the lattice oxygen of In_2O_3. O 1s (II) represents the oxygen vacancy state (anoxic state), which may come from the amorphous phase oxygen atom of ITO film or the oxygen atom bound by Sn atom[19–20]. Area ratios of O 1s (II) and O 1s (I) at various etching time are shown in Table 6. The relative change of binding energy of O 1s (I) and O 1s (II) indicates the change of oxygen vacancy concentration. When the etching time is short, the area of the oxygen region (O 1s(I)) is small, while the area of the anoxic region (O 1s (II)) is large. This indicates that the concentration of oxygen vacancies is large, and more oxygen vacancies promote the increase in carrier concentration, which is conducive to the decrease in resistivity. With the extension of etching time, the area of the lattice oxygen region (O 1s (I)) increases gradually. While the area of the hypoxia region (O 1s (II)) decreases gradually, indicating that the donor defect density decreases, which hinders the movement of carriers and reduces the carrier concentration, thus increasing the resistivity and decreasing the electrical performance of ITO films.

In combination with Fig.3, it is evident that for etching time within 40 h, there is only a small decrease in electrical properties of the ITO films. However, when the etching time exceeds 40 h, there is a significant decrease in electrical properties. This result is consistent with the changes in relative concentration of the In^{3+} and Sn^{4+} in the ITO films (Table 5). As the etching time increases, the In and Sn elements are unevenly distributed during sputtering, and the oxygen vacancies in the films decrease, degrading the electrical properties of the ITO films. For longer etching time, the target nodulation has a significant negative influence on the electrical properties.

2.2.2 Effects of etching time of ITO target on optical properties of ITO films

As can be seen from Fig. 9 and Fig. 10, the average light transmittance of the ITO films is over 90%, with very little change within 40 h, while it decreases rapidly above 40 h. Fig. 11 shows the SEM images of ITO films at different

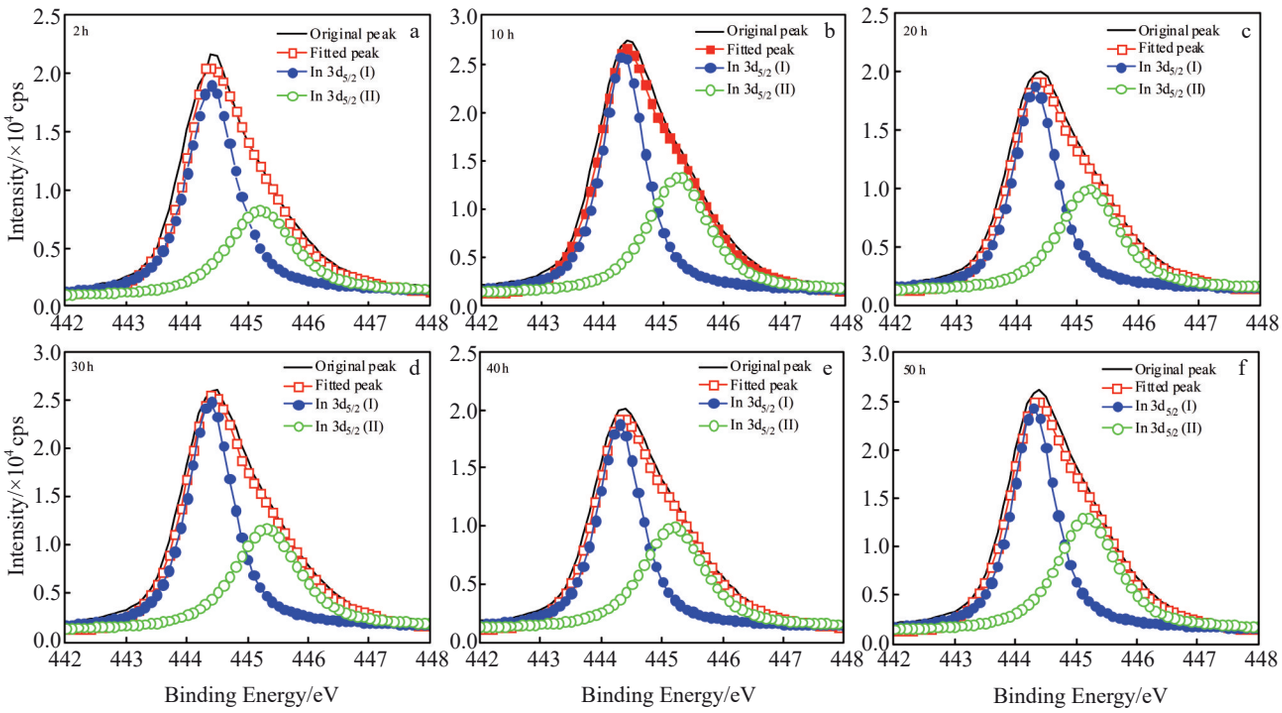

Fig.6 Peak-splitting and peak-fitting spectra of In $3d_{5/2}$ ITO films with various etching time: (a) 2 h, (b) 10 h, (c) 20 h, (d) 30 h, (e) 40 h, and (f) 50 h

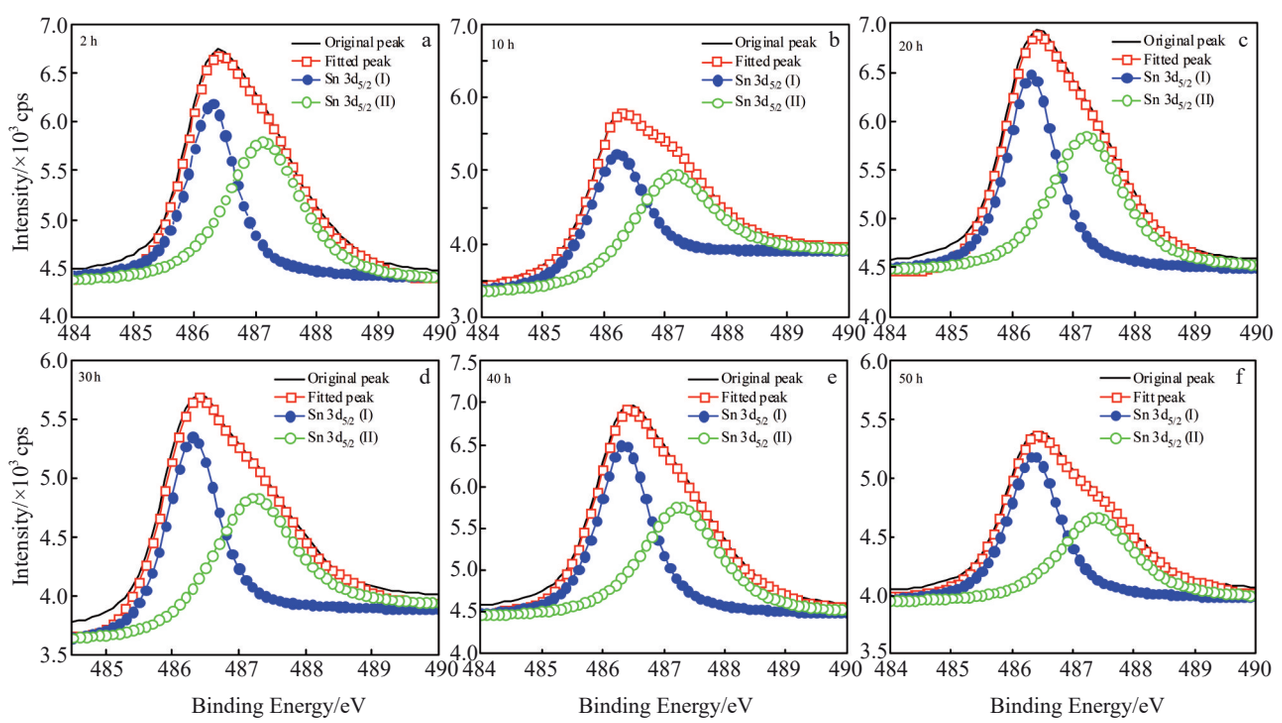

Fig.7 Peak-splitting and peak-fitting spectra of Sn $3d_{5/2}$ ITO films with various etching time: (a) 2 h, (b) 10 h, (c) 20 h, (d) 30 h, (e) 40 h, and (f) 50 h

Table 5 Relative content of In^{3+} and Sn^{4+} in ITO films with various etching time (%)

Element	Etching time/h					
	2	10	20	30	40	50
In^{3+}	35.2	38.7	41.5	41.8	43.1	44.7
Sn^{4+}	54.69	54.55	53.49	52.38	51.46	47.37

etching time. With the increase in etching time, the surface of ITO film gradually becomes rough. When the etching time is 40 h, crystal particle agglomeration occurs on the surface of ITO film. This may be related to the effect of the nodulation degree of target on the surface of ITO film. With the increase in etching time, the surface of the ITO target of nodules is serious, making the sputtered particles deposited on the

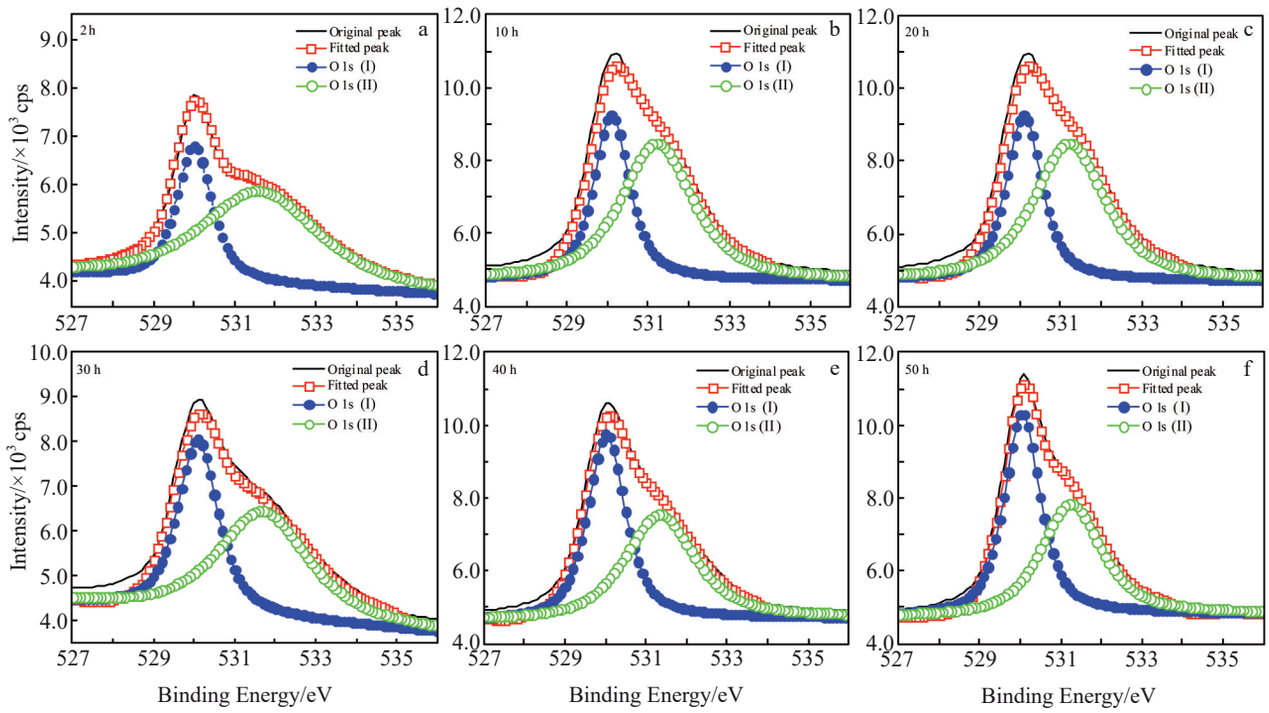

Fig.8 Peak-splitting and peak-fitting spectra of O 1s with various etching time: (a) 2 h, (b) 10 h, (c) 20 h, (d) 30 h, (e) 40 h, and (f) 50 h

Table 6 Area ratios of element O in ITO films in different states with various etching time

Area ratio	Etching time/h					
	2	10	20	30	40	50
$A_{O1s(II)}/A_{O1s(I)}$	1.09	0.945	0.726	0.694	0.658	0.437

substrate uneven and larger particles are sputtered out of the outer surface of thin film region. Consequently, more irregular structure forms and more crystal particles reunite together, making the film rough and inhomogeneous, increasing light scattering, and decreasing the transmittance of ITO film.

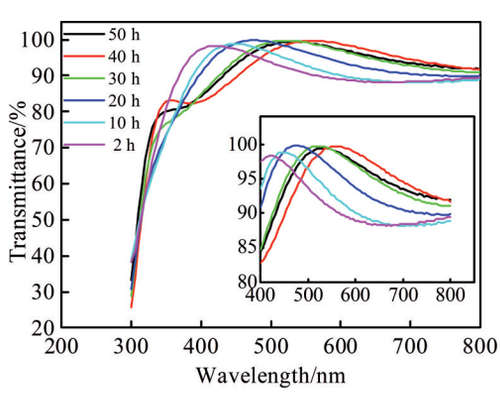

Fig.9 Optical transmittance spectra of ITO thin films with various etching time

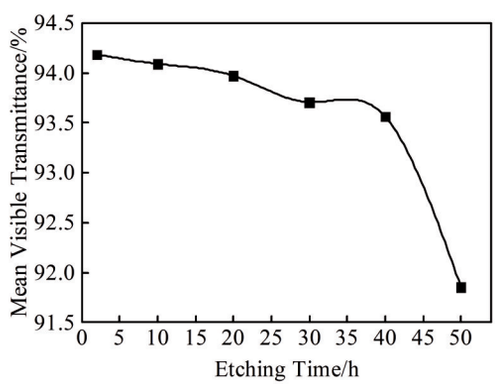

Fig.10 Mean visible transmittance of ITO films with various etching time

3 Conclusions

1) Substantial nodules appear on the surface of the ITO target at long etching time, resulting in uneven deposition of sputtering particles on the surface. Some large particles are sputtered out and thus irregular structures form on the depositing surface of the substrate, producing an uneven surface roughness that enhances the light scattering and decreases the light transmittance of the ITO films.

2) The photoelectric properties of the ITO films are strongly related to the etching time. With longer etching time, the distribution of In and Sn on the target surface is non-uniform, causing uneven distributions of In and Sn in the ITO films. The relative content of In^{3+} in the ITO films increases, while the relative content of Sn^{4+} decreases. As etching time increa-

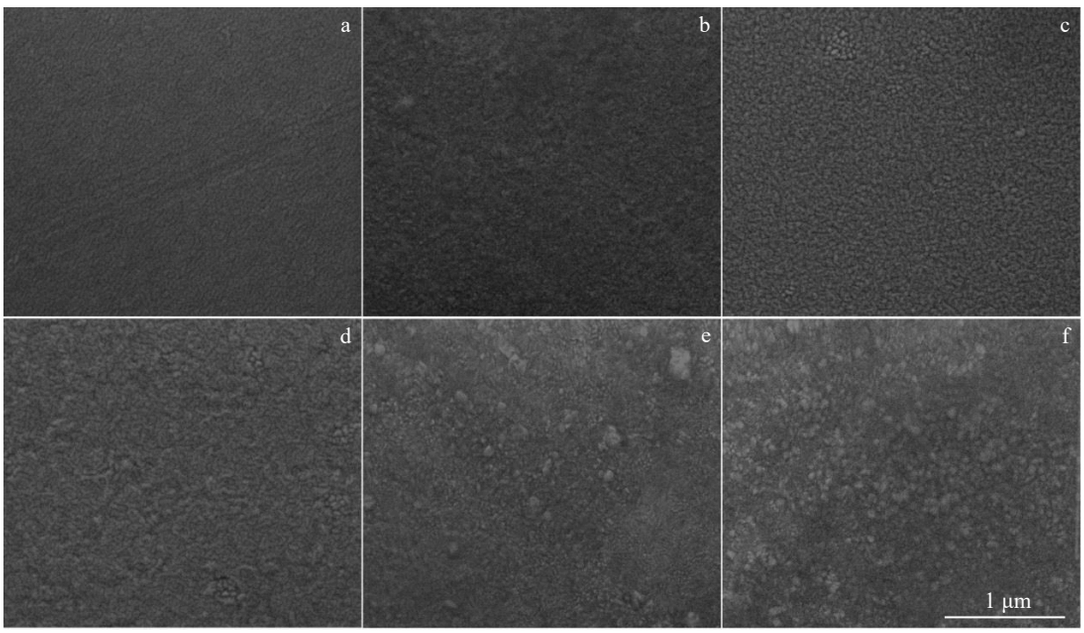

Fig.11 SEM images of surfaces of the ITO film with various etching time: (a) 2 h, (b) 10 h, (c) 20 h, (d) 30 h, (e) 40 h, and (f) 50 h

ses, the amount of oxygen vacancies in the ITO films decreases gradually, degrading their electrical performance. The light transmittance of the ITO films does not change significantly below etching time of 40 h, but decreases rapidly above 40 h.

References

1 Wang Guanjie, Wang Meihan, Wen Zhe *et al. Rare Metal Materials and Engineering*[J], 2022, 51(4): 1448
2 Xing Xiaoshuai, Liu Yingxia, Yu Xiaodong *et al. Rare Metal Materials and Engineering*[J], 2022, 51(2): 682
3 Cai Haichao, Xue Yujun, Li Hang *et al. Rare Metal Materials and Engineering*[J], 2021, 50(8): 2708
4 Wen F W, Bi S C. *Thin Solid Films*[J], 1997, 298: 221
5 Yang S, Zhong J, Sun B *et al. Journal of Materials Science: Materials in Electronics*[J], 2019, 30: 13 005
6 Yang S, Sun B, Liu Y *et al. Ceramics International*[J], 2020, 46: 6342
7 Nakashima K, Kumahara Y. *Vacuum*[J], 2002, 66: 221
8 Omata T, Kita M, Okada H *et al. Thin Solid Films*[J], 2006, 503: 22
9 Ishibashi S, Higuchi Y, Ota Y *et al. Journal of Vacuum Science & Technology A*[J], 1990, 8: 1403
10 Lippens P, Segers A, Haemers J *et al. Thin Solid Films*[J], 1998 317: 405
11 Liu C T, Lai M C, Hwang C C *et al. IEEE Transactions on Magnetics*[J], 2009, 45(10): 4391
12 Madsen N D, Christensen B H, Louring S *et al. Surface & Coatings Technology*[J], 2012, 206: 4850
13 Lippens P, Verheyen P. *Annual Technical Conference-Society of Vacuum Coaters*[C], 1994, 8–13: 254
14 John K A, Philip R R, Sajan P *et al. Vacuum*[J], 2016, 132: 91
15 Park J H, Buurma C, Sivananthan S *et al. Applied Surface Science*[J], 2014, 307: 388
16 Hu Y, Diao X, Wang C *et al. Vacuum*[J], 2004, 75: 183
17 Cui H N, Teixeira V, Meng L J. *Vacuum*[J], 2008, 82(12): 1507
18 Nadaud N, Lequeux N, Nanot M *et al. Journal of Solid State Chemistry*[J], 1998, 135: 140
19 Fan J C C, Goodenough J B. *Journal of Applied Physics*[J], 1977, 48: 3524
20 Major S, Kumar S, Bhatnagar M *et al. Applied Physics Letters*[J], 1986, 49: 394

ITO靶刻蚀时间对沉积ITO薄膜光电性能的影响

杨淑敏，谢 斌，张 伟，孔维静

(喀什大学 物理与电气工程学院，新疆 喀什 844006)

摘 要：在磁控溅射过程中，通过观察在2~50 h的刻蚀时间下制备的ITO薄膜的表面形貌，研究了在磁控溅射过程中ITO靶表面的黑色凸起的形成过程，并探讨了刻蚀时间对沉积ITO薄膜的光电性能的影响。结果表明，随着刻蚀时间的增长，ITO靶材表面的In和Sn分布发生变化，导致ITO膜不均匀。薄膜的电学和光学性能因结节的形成而显著退化。而当刻蚀时间在40 h以下时，ITO薄膜的光电性能变化不大。然而，当蚀刻时间继续延长，薄膜的光电性能会迅速恶化。

关键词：ITO靶材；ITO薄膜；结节；刻蚀时间；磁控溅射

作者简介：杨淑敏，女，1981年生，博士，教授，喀什大学物理与电气工程学院，新疆 喀什 844006，电话：0998-2309280，E-mail：shumin6666@126.com